http://journal.uir.ac.id/index.php/JGEET

E-ISSN : 2541-5794
P-ISSN : 2503-216X

Journal of Geoscience,
Engineering, Environment, and Technology
Vol 8 No 2 2023

RESEARCH ARTICLE

Morphological Analysis of Anak Krakatau Volcano after 22 December 2018 Eruption using Differential Interferometry Synthetic Aperture Radar (DInSAR)

Mochamad Iqbal[1], Anjar Dwi Asterina Denhi[2], Kristianto[3], Ardy Prayoga[3]

[1]*Petrology, Volcanology, and Geothermal Research Group, Geological Engineering, Institut Teknologi Sumatera, Way Huwi, South Lampung, 35365, Lampung, Indonesia.*

[2]*Geological Engineering, Institut Teknologi Sumatera, Jalan Terusan Ryacudu, Way Huwi, South Lampung, 35365, Lampung, Indonesia.*

[3]*Center for Volcanology and Geological Hazard Mitigation, Jalan Diponegoro No. 57 Bandung, 40122, Indonesia.*

* Corresponding author: mochamad.iqbal@gl.itera.ac.id
Tel.:+62 813 6652 7522
Received: Jan 5, 2023; Accepted: Mar 17, 2023.
DOI: 10.25299/jgeet.2023.8.2.11651

Abstract

Anak Krakatau Volcano is an active volcano located in the Krakatau Complex, Sunda Strait, Indonesia. On 22 December 2018, the volcano experienced a major eruption that led to a tsunami that devastated the shores of the islands of Java and Sumatra and killed up to 437 people. The eruption also destroyed the volcano's body and change its shape drastically and forming a large crater in the southwestern part. After that eruption, the volcano continues to grow up. This research aims to analyze the deformation of the Anak Krakatau Volcano post-2018 eruption by using the differential interferometry SAR method (DInSAR). In order to support the analysis, we additionally compare the DInSAR result with tectonic-volcanic activity. Sentinel 1-A type SLC satellite imagery data from 5 June 2019 to 7 January 2020; consisting of 19 images or 18 pairs as master and slave were used to producing a deformation map. DInSAR result shows the volcano was generally experiencing deflation during the period, ranging from -1.03 to -4.81 cm (-3.01 cm average). However, inflation also occurred ranging from 0 to 5.99 cm, correlating with shallow and deep volcanic activity and followed by eruptions in October 2019 when the highest activities were observed. Furthermore, coherence value should be highly considered along with DInSAR processing, and this research allows that coherence to be acceptable.

Keywords: Anak Krakatau Volcano, DInSAR, morphology, deformation.

1. Introduction

Anak Krakatau Volcano/Gunung Anak Krakatau (GAK) is an active volcano located in the Krakatau Complex, Sunda Strait, Indonesia (Fig 1). This volcano was formed several years after the eruption of the Krakatau volcano on 27 August 1883 which was one of the most violent volcanic eruptions in history and caused a tsunami (Jaxybulatov et al., 2011) with 36,000 death (Self, 1992). The eruption destroyed two-thirds of the Krakatau Volcano Island and form the remaining four small islands which became known as the Krakatau Complex: Anak Krakatau, Sertung, Panjang, and Rakata Island (Agustan et al., 2012). GAK sits directly on the boundary of the Indo-Australian and Eurasian tectonic plates, which are frequent regions of strong seismic and high volcanic activity (Babu and Kumar, 2019).

On 22 December 2018, there was an eruption of the Anak Krakatau volcano which triggered landslides in the western part of the mountain (Perttu et al., 2020; Williams et al., 2019). This event caused 437 fatalities, over 30 thousand injured, and thousands of houses destroyed. Several research has been conducted on the post-eruption that caused the tsunami, including tsunami modeling and morphological analysis using satellite imagery (Babu and Kumar, 2019; Grilli et al., 2019; Iqbal and Juliarka, 2020, 2019; Perttu et al., 2020; Williams et al., 2019). The Anak Krakatau volcano had a considerable morphological alteration following the eruption, creating a huge crater lake (Fig 2). Geochemically, after 2018 eruption, GAK composed of two groups, basaltic-andesitic composition, and the second group had lower SiO_2 and lower Al_2O_3 (Fiantis et al., 2021).

This study aims to analyze the morphology of GAK after the 2018 tsunami using the Differential Interferometry Synthetic Aperture Radar (DInSAR) method from Sentinel-1A satellite images from June 2019 to January 2020 combined with GAK eruption data. Coherence of InSAR and SAR backscatter images combined with high-resolution optical images could monitor surface deformation caused by volcanic eruptions (Babu and Kumar, 2019). Study of InSAR to detect volcanoes morphological changes was provenly effective in such studies (Antonielli et al., 2014; Astort et al., 2022; De Novellis et al., 2017), furthermore to detect the changes of shallow magma reservoir (Euillades et al., 2017; Sreejith et al., 2020). To verify the results obtained through displacement and phase analysis at the DInSAR stage, deformation monitoring was carried out before and after the eruption of Anak Krakatau.

2. Data and Methods

2.1. Data

The data used in this study are Sentinel-1A imagery in IW mode of SLC type with ascending directions to observe the deformation that occurred during that period. This research is also supported by secondary data in the form of GAK volcanic earthquake data, namely the number of eruptions/eruption activities, blow, shallow volcanic, deep volcanic, local tectonics, and deep tectonics obtained from the Center for Volcanology and Hazard Mitigation Indonesia (CVGHM). Sentinel-1A data processing was performed using the SNAP software with data downloaded on NASA's EARTHDATA (https://search.asf.alaska.edu/).

Sentinel 1-A type SLC satellite imagery data has a 12-day repeating cycle to return to the initial orbit, so the timeframe for this research is taken every 12 days starting from June 2019 to January 2020. Images are processed in pairs from the oldest date and will become the master while the latter data on the 12th day will become a slave. This short period aims to accurately determine deformation values because Sentinel-1 has a C-band sensor that can penetrate vegetation up to 6 cm (Putri et al., 2018). With two satellite images that have the same area, the same orbit, and the same geometry, an interferogram was created which represents the deformation or surface changes between the two SAR data generated by calculating the difference in the phases of the 2 products. The process was repeated for each pair of master and slave data and produced deformation maps. The pairs of Sentinel-1A images used in this study can be seen in Table 1. The data is using VV polarization and orbit at 171.

Table 1. Master and slave date acquired at ascending direction.

Pair Number or Period	Master	Slave
1	05/06/2019	17/06/2019
2	17/06/2019	29/06/2019
3	29/06/2019	11/07/2019
4	11/07/2019	23/07/2019
5	23/07/2019	04/08/2019
6	04/08/2019	16/08/2019
7	16/08/2019	28/08/2019
8	28/08/2019	09/09/2019
9	09/09/2019	21/09/2019
10	21/09/2019	03/10/2019
11	03/10/2019	15/10/2019
12	15/10/2019	27/10/2019
13	27/10/2019	08/11/2019
14	08/11/2019	20/11/2019
15	20/11/2019	02/12/2019
16	02/12/2019	14/12/2019
17	14/12/2019	26/12/2019

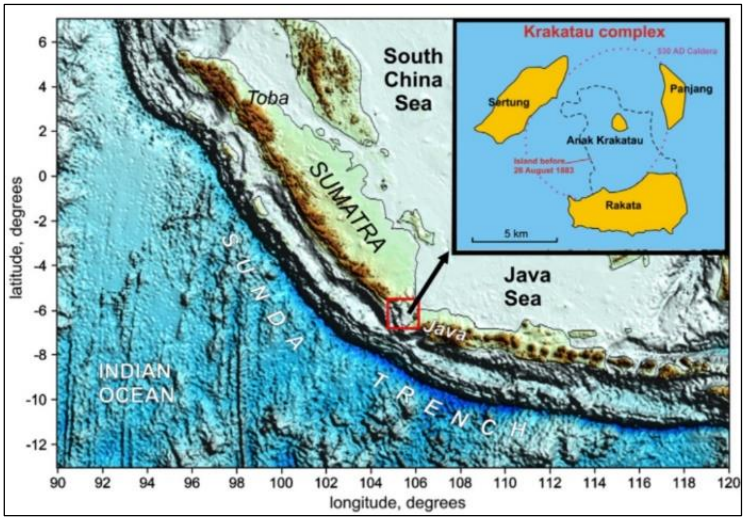

Fig 1. Krakatau Volcanic Complex (Jaxybulatov et al., 2011)

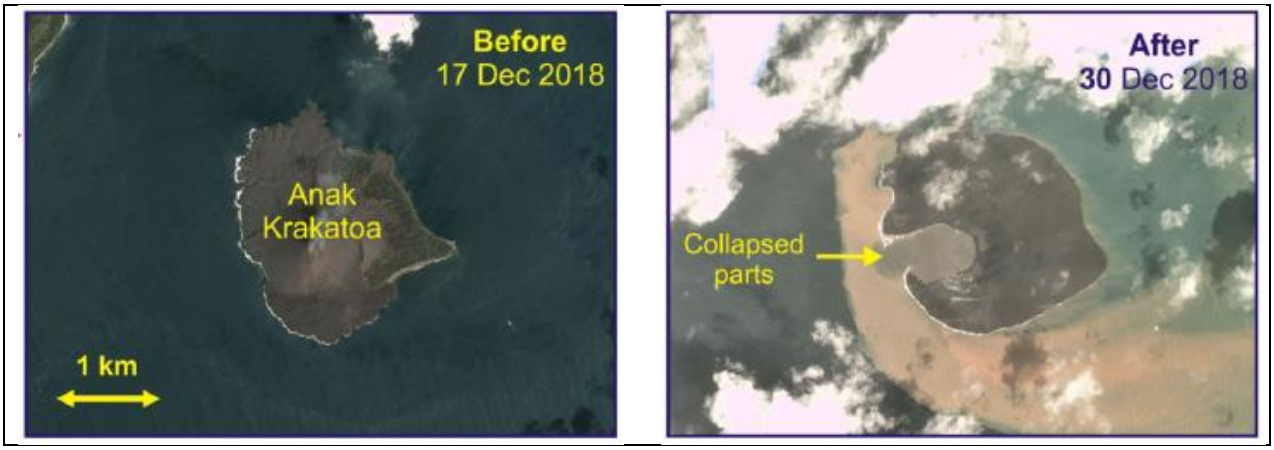

Fig 2. GAK morphology changed after the eruption on December 22, 2018 (Heidarzadeh et al., 2020).

2.2. Method

Differential Interferometry Synthetic Aperture Radar (DInSAR) is a radar-based method that utilizes the phase differences of two or more SAR images with different acquisition times and the same area in their processing to obtain deformation values in an area (Castañeda et al., 2011). In general, the steps of DInSAR are described in Figure 3. Data processing is carried out from paired data to produce deformation images to be analyzed.

A pair of Sentinel-1A images that have been downloaded are input into the SNAP software with one image as the *master* image which has the earlier acquisition date, and the other image as the *slave* image which has the later acquisition. The Sentinel-1A imagery used in this study uses the IW (interferometric wide swath) recording mode with an area of 250 km and a spatial resolution of 5 m to 20 m. Therefore, the *TOPSAR split process* (image cropping) is carried out according to the research area. The GAK subswath is located in IW3. VV polarization is used to see the vertical change from

the top of the GAK to the surface boundary. The image that has been registered through the *apply orbit file* stage then be carried out to form an interferogram. The *back geocoding* process produces an altitude model product (Digital Elevation Model) which is acquired through a combination of two master and slave radar data. *Enhanced Spectral Diversity* serves to improve the accuracy of the DEM *coregistration* process resulting from back geocoding by correcting the azimuth direction and range of each bar. The image that has improved accuracy can then start *Interferogram Formation Processing* which can produce an interferogram phase originating from a combination of the master image and the slave image. The coherence relationship between the master and slave images in each pixel of the slave image to the master image, if the value is close to one then the image will approach the master image and it can be said that the two images are very identical, or could be said has high accuracy. The latest noise interferogram products can be removed through the *TopSAR Deburst* process. *Topographic phase removal* is used to remove topographical effects on the phase and make it flat to the projection plane. Furthermore, *Multilooking* functions to reduce the standard deviation of the noise level as well as the resolution and pixel size of the product resulting from the Topographic phase removal. Disorders that exist after the DInSAR process are filtered on *Goldstein phase filtering*. The *phase unwrapping* process functions to change the phase units from radians to metrics. DEM with 3Sec SRTM type will slightly speed up the unwrapping process. The result of this processing is the vertical displacement value of LOS (Line of Sight) in the negative to the positive range which has units of meters. A negative value reflects deflation and if the value is positive then the surface is experiencing inflation. Then, the *geometric correction* stage is carried out to avoid geometric distortion of the distorted image. The last step is a subset to limit the resulting image according to the size of the area we have determined.

The results of DInSAR processing show the value of the absolute deformation rate with units of meters to centimeters. These values are then visualized in the form of GAK deformation maps to describe the distribution of inflation and deflation that occur. Based on the processing results formed, we can compare with data on the number of earthquake activities in the form of eruptions, gas blow, and deep and shallow volcanic earthquakes and compare with geological data in the form of related structures and lithology, so that the possible causes of inflation and deflation on the volcano can be identified.

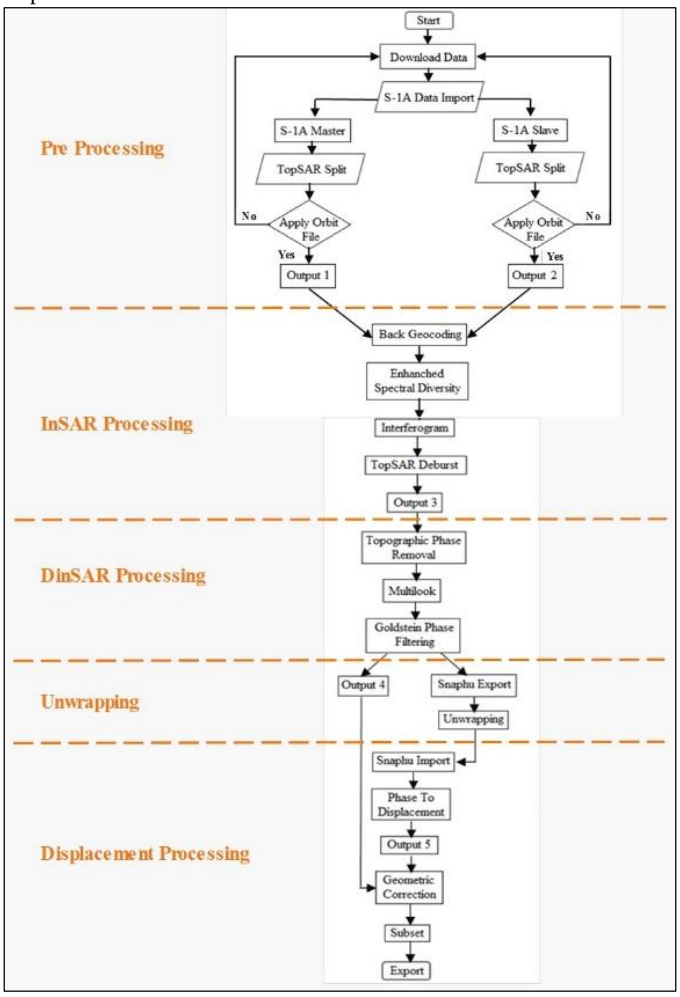

Fig 3. DInSAR processing stages.

3. Result and Discussion

3.1. Deformation

Deformation during the observation period was observed only at GAK and is related to volcanic activity. The surface pattern of deformation from June 2019 to early January 2020 shows low LOS changes (deflation or subsidence) shown in dark blue and accompanied by high LOS (inflation or uplift) shown in red in Figure 4. The changes in the volcano's body volume could be an indicator of the volcanic eruption (Abdurrachman et al., 2018).

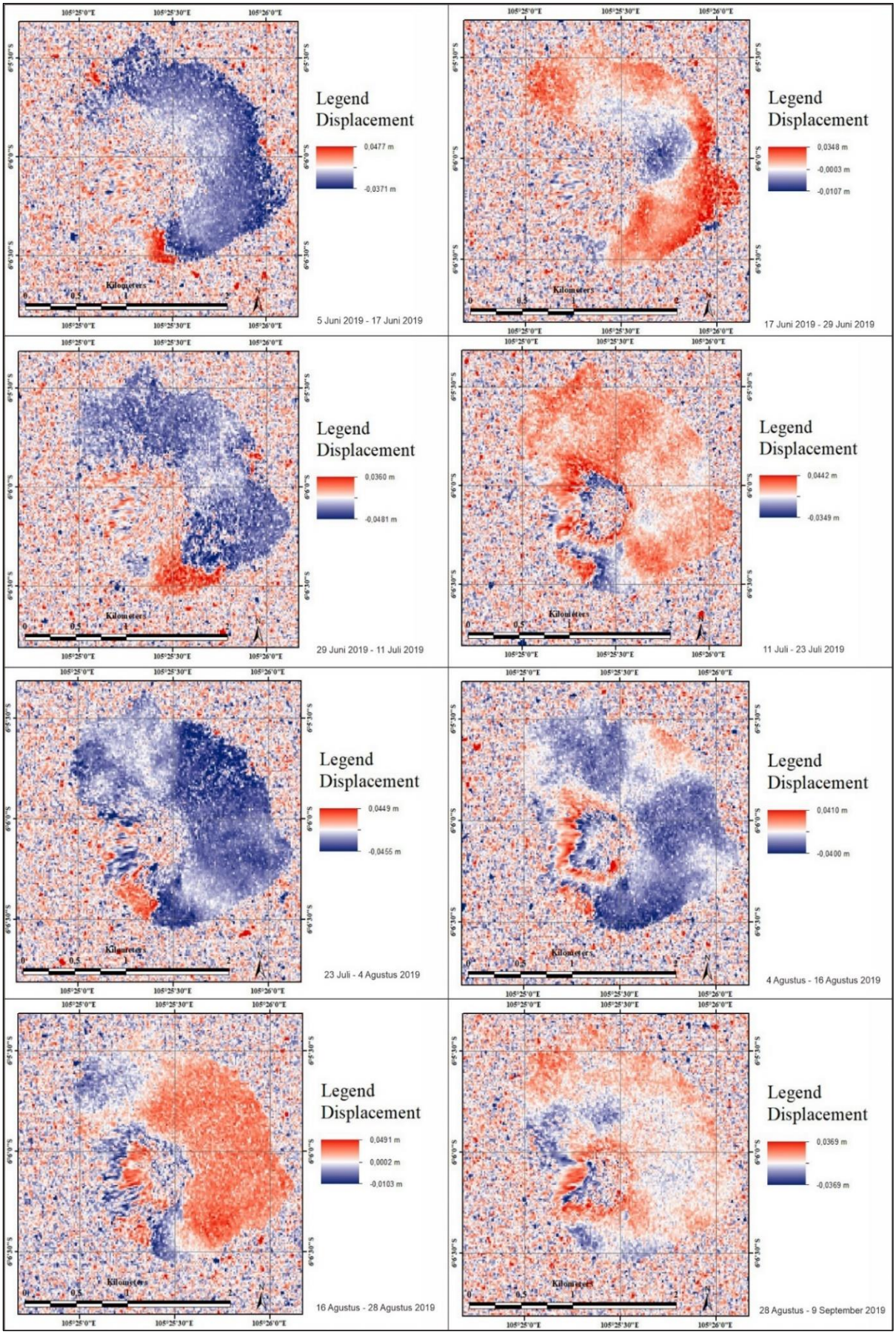

Fig 4. GAK deformation pattern, Noted that blue color is relatively deflating while red shows inflation.

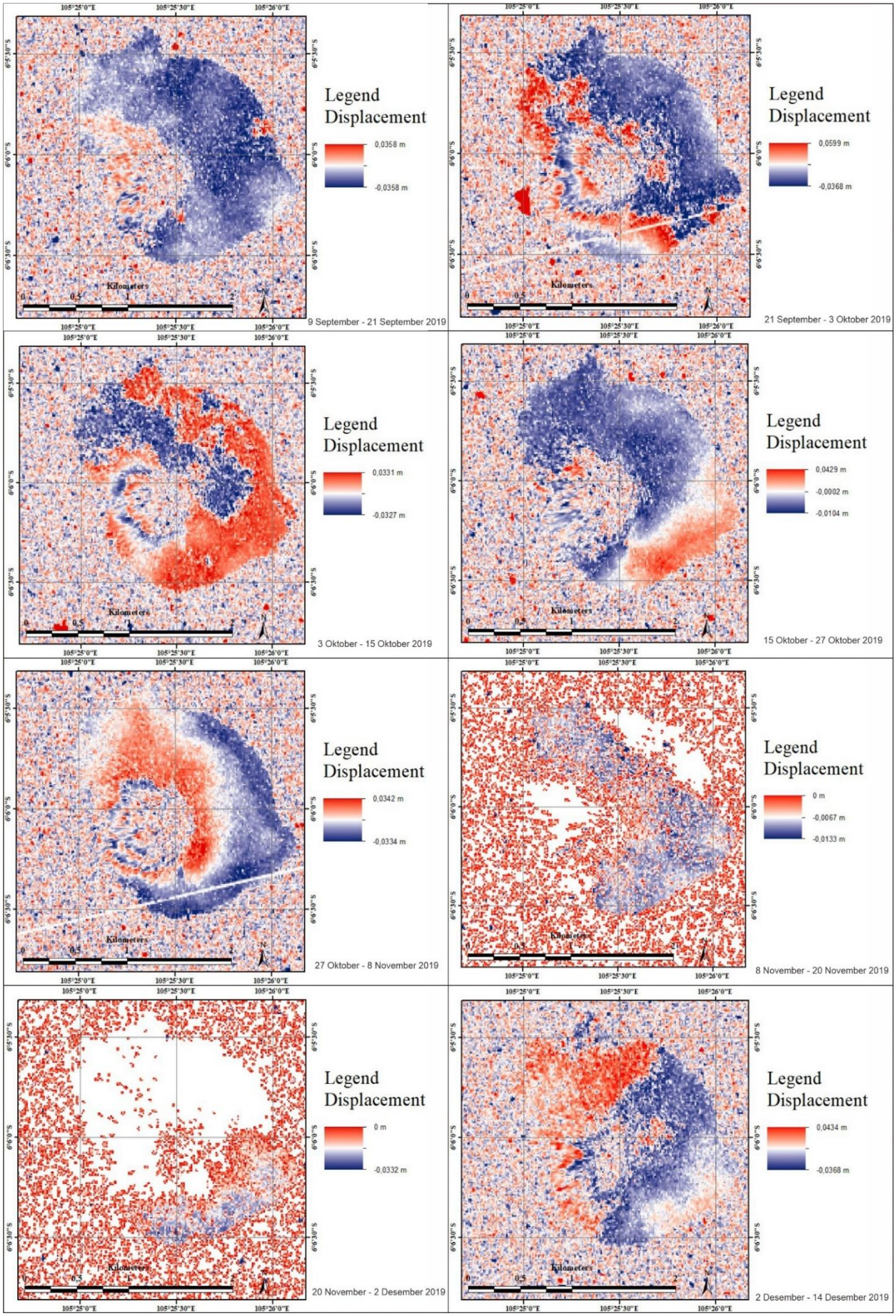

Fig 4. (continue) GAK deformation pattern. Noted that blue color is relatively deflating while red showing inflation.

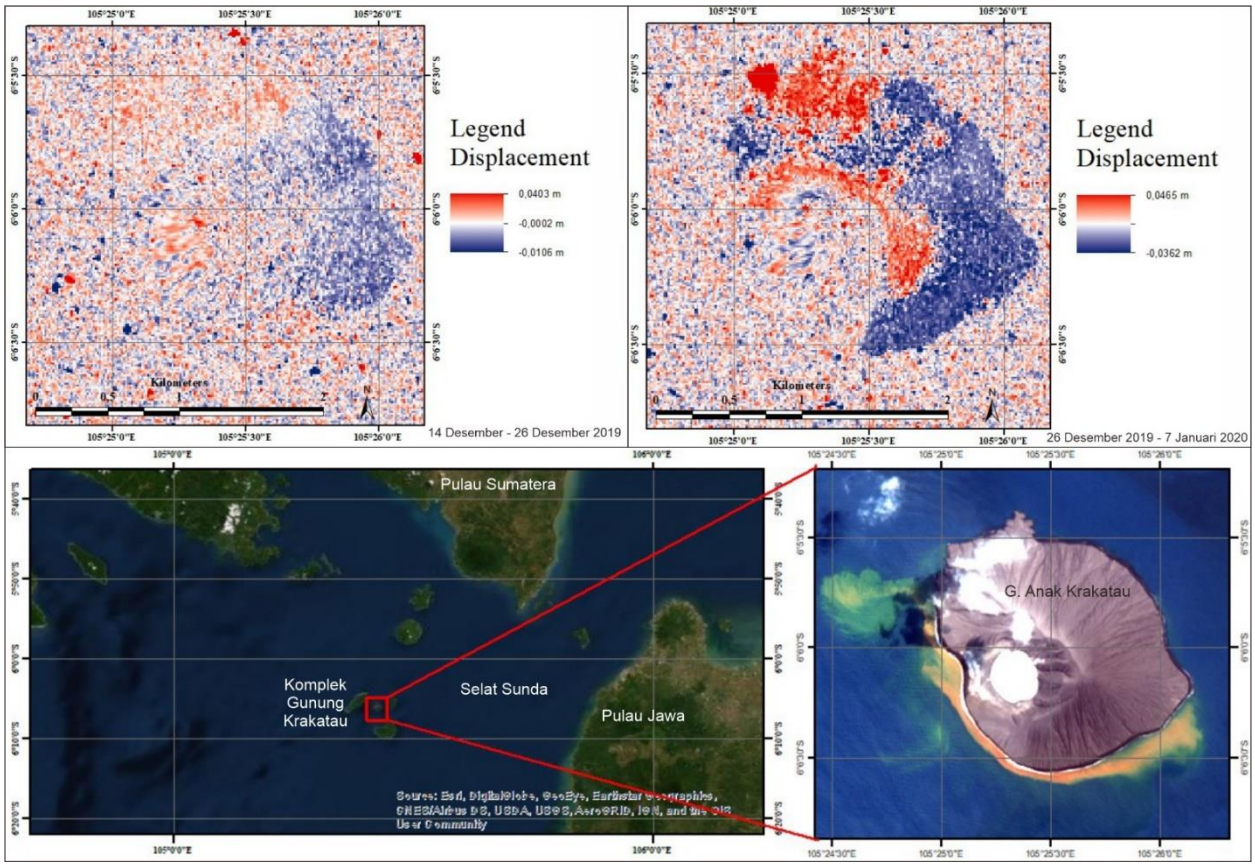

Fig 4. (continue) GAK deformation pattern. Noted that blue color is relatively deflating while red shows inflation.

The distribution and morphological changes of GAK were not uniform in each period, some experienced deflation with a wide pattern, but with a low deflation rate, and vice versa so did the inflation rate. This is because changes in GAK morphology are determined by various factors such as tectonic activity, volcanoes, eruptions, geological structures, etc. However, in general, the deformation pattern from the Ascending LOS profile from June 2019 to early January 2020 shows a dominant deflation which is likely due to ongoing earthquake activity and shallow magma sources (Agustan et al., 2012; Harjono et al., 1989). The correlation between GAK activity and maximum deformation is depicted in Figure 5. The spatial distribution of the deformations can be observed in Figure 4 and can be compared with the deformation values that occur in Figure 5.

Generally, the tectonic activity that occurs in GAK is relatively low, namely from 1-4 events, both local and distant tectonics. Shallow and deep volcanic activity has a higher frequency, from 1-12 events, and occurs almost every day. Meanwhile, eruptions occur almost every day with the highest frequency occurring on 12 October 2019, which is 43 times.

According to the summary of deformations that occurred in GAK (Figure 5), the maximum inflation value that occurred in each period was considerably uniform, specifically in the range of 3.31 to 5.99 cm (with an average of 3.72 cm), except for the period from 8 September to 2 December 2019, when there was no positive deformation. In contrast, GAK has considerably less deflating or subsidence, with a maximum of -1.03 to -4.81 cm and an average of -3.01 cm over each period. The occurrence of morphological changes, in general, is not determined by these maximum inflation and deflation values, but these values must be compared with the spatial distribution of morphological changes in Figure 4.

From Figure 5 it can be seen that volcanic activity reached its peak in October 2019, when both shallow and deep volcanic activity occurred accompanied by an increase in daily eruptions. This is also supported by the dominant distribution of inflation (marked in red color) in the DInSAR period 3-15 October 2019 (Figure 4). It should be noted that the high activity of gas emission in the November 2019 period from GAK will only slightly affect the morphology of GAK because it is not followed by the deposition of pyroclastic material.

3.2. DInSAR accuracy

The accuracy of DInSAR processing could be reflected in its coherence. The results of the DInSAR process have a coherence value with a range of values from 0 – 1. If the coherence value = 1 indicates that the master and slave images on the interferogram are completely identical, and vice versa with a coherence value = 0. The higher the coherence value, it means the accuracy is also high, and the contrary (Hooper et al., 2004; Kurniawan and Anjasmara, 2016). Here we obtain the coherence profile from the 1st period (Figure 6a) and the 18th period (Figure 6b). The figures show both results have a good value of coherence around the volcano, the shape of the volcanoes could be clearly seen and reflected by the white color (high values of coherence). Comparing two datasets with a short time gap is the ideal approach to maintain DInSAR accuracy. A long temporal resolution will cause poor DInSAR coherence. Furthermore, to obtain coherence from the first to the last period, we combine/overlay Figures 6a and 6b. Despite the fact that the coherence is diminishing in some areas, such as the western flank and crater area, the form of GAK is still recognizable, and the outcome is still acceptable.

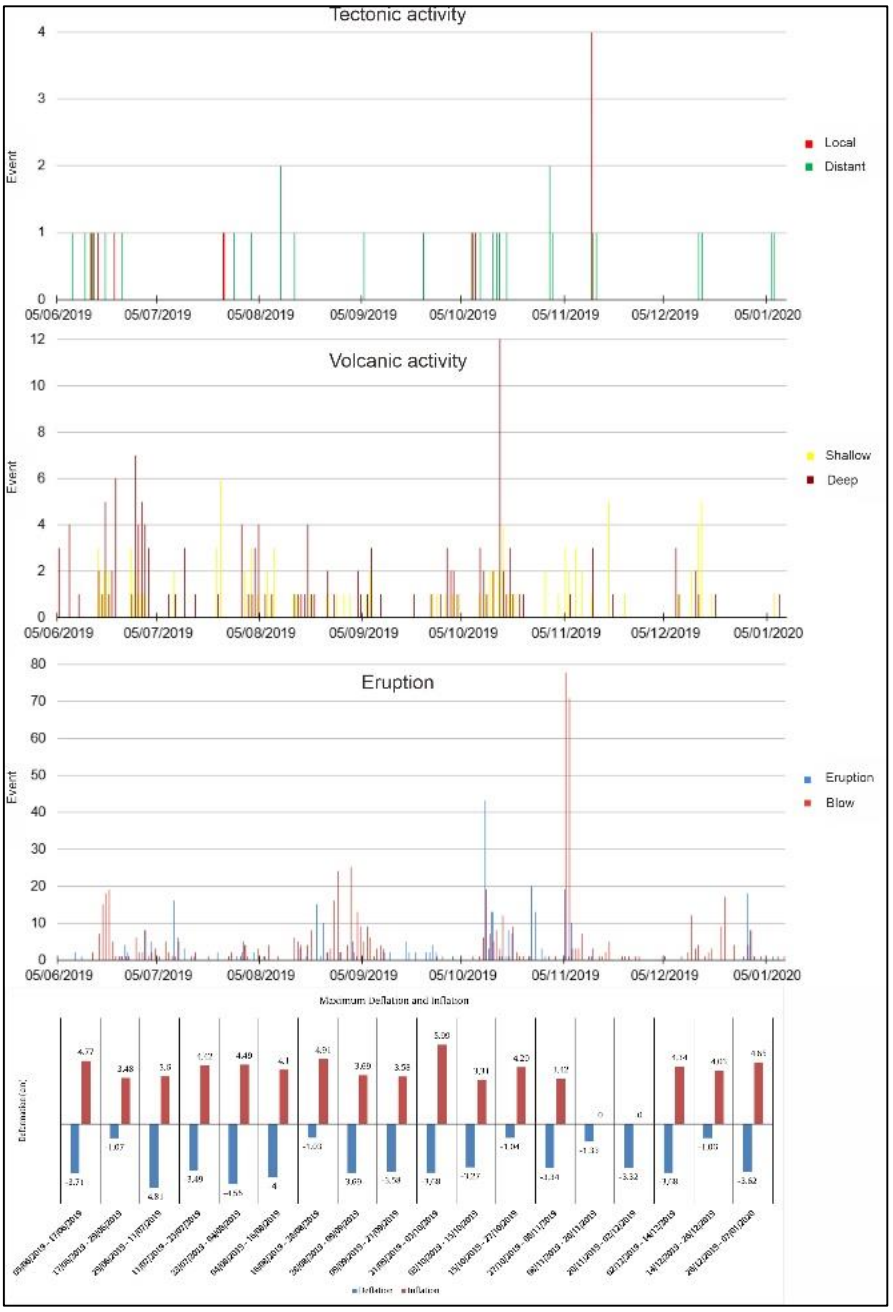

Fig 5. GAK activities during DInSAR processing period.

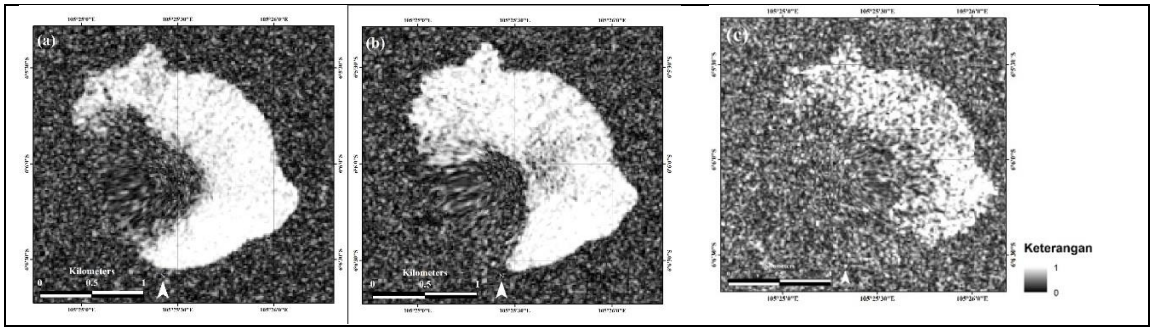

Fig 6. GAK Coherence Profile (a) Period 5 - 17 June 2019 (b) Period 26 December - 07 January 2020 (c) Combination of a and b. White color means high coherence; black color means low coherence.

4. Conclusion

The eruption of the Anak Krakatau volcano (GAK) on December 2018 drastically change its shape and form a large crater southwest of the body. This research combines synthetic aperture radar image and volcano-tectonic activity and then analyzes the changes in morphology with the DInSAR method. Post-eruption, GAK is showing alteration of morphology dominated by deflating with a range of -1.03 to -4.81 cm

(averagely -3.01 cm) within the 5th June 2019 to 7th January 2020 period.

On the other hand, GAK also suffers from inflating with a range from 0 to 5.99 cm (average 3.72 cm). The peak of positive deformation occurred when GAK is highly active in October 2019 when shallow and deep volcanic activity happen and followed by an eruption.

A combination of DInSAR and volcanic activity could successfully detect the changes in volcanic morphology and probably could detect future eruption. However, the coherence of DInSAR processing should be highly taken into consideration. This DInSAR method is probably the traditional method to conduct. A new and more sophisticated method such as Persistent Scatterer InSAR (PS-InSAR), Small Baseline Subset (SBAS) InSAR, or the other time-series InSAR could achieve a better result.

Acknowledgments

The author would like to thank the Center for Volcanology and Geological Hazard Mitigation (CVGHM) for assistance in obtaining data on the number of earthquake activities in the Anak Krakatau Volcano area which was very valuable for the additional data on this research.

References

Abdurrachman, M., Widiyantoro, S., Priadi, B., Ismail, T., 2018. Geochemistry and Structure of Krakatoa Volcano in the Sunda Strait, Indonesia. Geosciences 8, 111. https://doi.org/10.3390/geosciences8040111

Agustan, Kimata, F., Pamitro, Y.E., Abidin, H.Z., 2012. Understanding the 2007–2008 eruption of Anak Krakatau Volcano by combining remote sensing technique and seismic data. International Journal of Applied Earth Observation and Geoinformation 14, 73–82. https://doi.org/10.1016/j.jag.2011.08.011

Antonielli, B., Monserrat, O., Bonini, M., Righini, G., Sani, F., Luzi, G., Feyzullayev, A.A., Aliyev, C.S., 2014. Pre-eruptive ground deformation of Azerbaijan mud volcanoes detected through satellite radar interferometry (DInSAR). Tectonophysics 637, 163–177. https://doi.org/10.1016/j.tecto.2014.10.005

Astort, A., Boixart, G., Folguera, A., Battaglia, M., 2022. Volcanic unrest at Nevados de Chillán (Southern Andean Volcanic Zone) from January 2019 to November 2020, imaged by DInSAR. Journal of Volcanology and Geothermal Research 427, 107568. https://doi.org/10.1016/j.jvolgeores.2022.107568

Babu, A., Kumar, S., 2019. InSAR Coherence and Backscatter Images Based Analysis for the Anak Krakatau Volcano Eruption. Proceedings 24, 21. https://doi.org/10.3390/IECG2019-06216

Castañeda, C., Pourthie´, N., Souyris, J.-C., 2011. Dedicated SAR interferometric analysis to detect subtle deformation in evaporite areas around Zaragoza, NE Spain. International Journal of Remote Sensing 32, 1861–1884. https://doi.org/10.1080/01431161003631584

De Novellis, V., Castaldo, R., De Luca, C., Pepe, S., Zinno, I., Casu, F., Lanari, R., Solaro, G., 2017. Source modelling of the 2015 Wolf volcano (Galápagos) eruption inferred from Sentinel 1-A DInSAR deformation maps and pre-eruptive ENVISAT time series. Journal of Volcanology and Geothermal Research, Volcano Geodesy: Recent developments and future challenges 344, 246–256. https://doi.org/10.1016/j.jvolgeores.2017.05.013

Euillades, P.A., Euillades, L.D., Blanco, M.H., Velez, M.L., Grosse, P., Sosa, G.J., 2017. Co-eruptive subsidence and post-eruptive uplift associated with the 2011–2012 eruption of Puyehue-Cordón Caulle, Chile, revealed by DInSAR. Journal of Volcanology and Geothermal Research, Volcano Geodesy: Recent developments and future challenges 344, 257–269. https://doi.org/10.1016/j.jvolgeores.2017.06.023

Fiantis, D., Ginting, F.I., Seprianto, Halfero, F., Saputra, A.P., Nelson, M., Van Ranst, E., Minasny, B., 2021. Geochemical and mineralogical composition of the 2018 volcanic deposits of Mt. Anak Krakatau. Geoderma Regional 25, e00393. https://doi.org/10.1016/j.geodrs.2021.e00393

Grilli, S.T., Tappin, D.R., Carey, S., Watt, S.F.L., Ward, S.N., Grilli, A.R., Engwell, S.L., Zhang, C., Kirby, J.T., Schambach, L., Muin, M., 2019. Modelling of the tsunami from the December 22, 2018 lateral collapse of Anak Krakatau volcano in the Sunda Straits, Indonesia. Scientific Reports 9, 11946. https://doi.org/10.1038/s41598-019-48327-6

Harjono, H., Diament, M., Nouaili, L., Dubois, J., 1989. Detection of magma bodies beneath Krakatau volcano (Indonesia) from anomalous shear waves. Journal of Volcanology and Geothermal Research 39, 335–348. https://doi.org/10.1016/0377-0273(89)90097-8

Heidarzadeh, M., Ishibe, T., Sandanbata, O., Muhari, A., Wijanarto, A.B., 2020. Numerical modeling of the subaerial landslide source of the 22 December 2018 Anak Krakatoa volcanic tsunami, Indonesia. Ocean Engineering 195, 106733. https://doi.org/10.1016/j.oceaneng.2019.106733

Hooper, A., Zebker, H., Segall, P., Kampes, B., 2004. A new method for measuring deformation on volcanoes and other natural terrains using InSAR persistent scatterers. Geophysical Research Letters 31. https://doi.org/10.1029/2004GL021737

Iqbal, M., Juliarka, B.R., 2020. Identification of Permeability Level by using Fault Fracture Density Analysis and Landsat 8 OLI at Ulubelu Geothermal Area. IOP Conf. Ser.: Earth Environ. Sci. 537, 012016. https://doi.org/10.1088/1755-1315/537/1/012016

Iqbal, M., Juliarka, B.R., 2019. Analisis Kerapatan Kelurusan (Lineament Density) di Lapangan Panasbumi Suoh-Sekincau, Lampung. Journal of Science and Applicative Technology 3, 61–67. https://doi.org/10.35472/jsat.v3i2.212

Jaxybulatov, K., Koulakov, I., Seht, M.I., Klinge, K., Reichert, C., Dahren, B., Troll, V.R., 2011. Evidence for high fluid/melt content beneath Krakatau volcano (Indonesia) from local earthquake tomography. Journal of Volcanology and Geothermal Research 206, 96–105. https://doi.org/10.1016/j.jvolgeores.2011.06.009

Kurniawan, R., Anjasmara, I.M., 2016. Pemanfaatan Metode Differential Intermerometry Synthetic Aperture Radar (DInSAR) untuk Pemantauan Deformasi Akibat Aktivitas Eksploitasi Panasbumi. Jurnal Teknik ITS 5, B331–B336. https://doi.org/10.12962/j23373539.v5i2.17361

Perttu, A., Caudron, C., Assink, J.D., Metz, D., Tailpied, D., Perttu, B., Hibert, C., Nurfiani, D., Pilger, C., Muzli, M., Fee, D., Andersen, O.L., Taisne, B., 2020. Reconstruction of the 2018 tsunamigenic flank collapse and eruptive activity at Anak Krakatau based on eyewitness reports, seismo-acoustic and satellite observations. Earth and Planetary Science Letters 541, 116268. https://doi.org/10.1016/j.epsl.2020.116268

Putri, D.R., Sukmono, A., Sudarsono, B., 2018. ANALISIS KOMBINASI CITRA SENTINEL-1A DAN CITRA SENTINEL-2A UNTUK KLASIFIKASI TUTUPAN LAHAN (STUDI KASUS: KABUPATEN DEMAK,

JAWA TENGAH). Jurnal Geodesi UNDIP 7, 85–96.
Self, S., 1992. Krakatau revisited: The course of events and interpretation of the 1883 eruption. GeoJournal 28, 109–121. https://doi.org/10.1007/BF00177223
Sreejith, K.M., Agrawal, R., Agram, P., Rajawat, A.S., 2020. Surface deformation of the Barren Island volcano, Andaman Sea (2007–2017) constrained by InSAR measurements: Evidence for shallow magma reservoir and lava field subsidence. Journal of Volcanology and Geothermal Research 407, 107107. https://doi.org/10.1016/j.jvolgeores.2020.107107
Williams, R., Rowley, P., Garthwaite, M.C., 2019. Reconstructing the Anak Krakatau flank collapse that caused the December 2018 Indonesian tsunami. Geology 47, 973–976. https://doi.org/10.1130/G46517.1